AI ensemble for signal detection of higher order gravitational wave modes of quasi-circular, spinning, non-precessing binary black hole mergers

Minyang Tian

Data Science and Learning Division,
Argonne National Laboratory,
Lemont, Illinois 60439, USA
Department of Physics & NCSA,
University of Illinois at Urbana-Champaign,
Urbana, Illinois 61801, USA
mtian8@illinois.edu

E. A. Huerta

Data Science and Learning Division,
Argonne National Laboratory,
Lemont, Illinois 60439, USA
Department of Computer Science
The University of Chicago,
Chicago, Illinois 60637, USA
elihu@{anl.gov,uchicago.edu}

Huihuo Zheng

Leadership Computing Facility, Argonne National Laboratory, Lemont, Illinois 60439, USA huihuo.zheng@anl.gov

Abstract

We introduce spatiotemporal-graph models that concurrently process data from the twin advanced LIGO detectors and the advanced Virgo detector. We trained these AI classifiers with 2.4 million IMRPhenomXPHW veforms that describe quasi-circular, spinning, non-precessing binary black hole mergers with component masses $m_{\{1,2\}} \in [3M \circ, 50M \circ]$, and individual spins $s_{\{1,2\}}^z \in [-0.9, 0.9]$; and which include the $(\ell, |m|) = \{(2, 2), (2, 1), (3, 3), (3, 2), (4, 4)\}$ modes, and mode mixing effects in the $\ell = 3$, |m| = 2 harmonics. We trained these AI classifiers within 22 hours using distributed training over 96 NVIDIA V100 GPUs in the Summit supercomputer. We then used transfer learning to create AI predictors that estimate the total mass of potential binary black holes identified by all AI classifiers in the ensemble. We used this ensemble, 3 classifiers for signal detection and 2 total mass predictors, to process a year-long test set in which we injected 300,000 signals. This year-long test set was processed within 5.19 minutes using 1024 NVIDIA A100 GPUs in the Polaris supercomputer (for AI inference) and 128 CPU nodes in the ThetaKNL supercomputer (for post-processing of noise triggers), housed at the Argonne Leadership Computing Facility. These studies indicate that our AI ensemble provides state-of-the-art signal detection accuracy, and reports 2 misclassifications for every year of searched data. This is the first AI ensemble designed to search for and find higher order gravitational wave mode signals.

1 Introduction

Artificial Intelligence (AI) applications have led to remarkable breakthroughs in science, engineering, industry, and tech during the last decade [1]. Novel AI applications are now being explored in earnest to address contemporary scientific grand challenges, as well as to provide a platform to elevate human insight across disciplines [2, 3]. Gravitational wave astrophysics is part of this revolution. For several

years now, an ever growing, international community of researchers has been developing novel AI tools to maximize the science reach of gravitational wave astrophysics [4–7]. In this article, we contribute to the development of AI to search for and find higher order gravitational wave modes emitted by quasi-circular, spinning, non-precessing, stellar mass binary black hole mergers.

Assumptions. We consider a three detector network comprising the advanced LIGO Livingston (L) and Hanford (H) detectors, and advanced Virgo (V). We train, validate and test our AI models using modeled waveforms that include higher order gravitational wave modes, and mode mixing effects. We use colored Gaussian noise throughout this analysis to benchmark this approach. In future work we will extend this analysis using real gravitational wave noise. To model the sensitivity of our proposed three detector network, we use the following target power spectral density (PSD) noise curves: aligo_O4high.tx for the advanced LIGO detectors, and avirgo_O5low_NEW.txt for advanced Virgo [8, 9]. We do this to consider gravitational wave detectors with comparable sensitivity.

Claims. To the best of our knowledge, we present the first AI models in the literature trained for signal detection of higher order gravitational wave modes emitted by quasi-circular, spinning, non-precessing binary black hole mergers. We quantified the performance of these AI models for signal detection by processing a year of coloured Gaussian noise in which we injected 300,000 higher order gravitational wave mode signals. Using the Receiver Operating Characteristic Area Under the Curve (ROC AUC), and the Precision Recall Area Under the Curve (PR AUC), we found that our AI classifiers provide state-of-the-art signal detection accuracy, and report 3 false positives over a year's long test set. Once we post-processed noise triggers with 2 AI total mass predictors, we reduced the number of misclassifications to only 2 over an entire year of searched data.

Limitations. Our AI models have been designed assuming a three detector network, LHV. We will explore larger detector networks in future work. Our AI models have been trained, validated and tested using coloured Gaussian noise, and target PSDs for the sensitivity of the LHV network. This is done to understand the performance of our AI models with controlled experiments, and to develop the required scientific software to handle these large datasets, and to train models at scale. In future work we will leverage this knowledge and scientific software to develop new AI models using gravitational wave data from the Gravitational Wave Open Science Center [10].

Reproducibility. We release our AI models, along with a tutorial that provides a step-by-step guide to use them, in the following GitHub repository: https://github.com/mtian8/Higher_Order_GW_Spatiotemporal_GNN

2 Methods

Datasets. We produced a set of 3 million waveforms with the IMRPhenomXPhh roximant [11]. These modeled waveforms are one second long, sampled at 4096 Hz, and describe quasicircular, spinning, non-precessing binary black hole mergers with component masses $m_{\{1,2\}} \in [3M_{\odot}, 50M_{\odot}]$, and individual spins $s_{\{1,2\}}^z \in [-0.9, 0.9]$; and which include the $(\ell, |m|) = \{(2, 2), (2, 1), (3, 3), (3, 2), (4, 4) \text{ modes}$, and mode mixing effects in the $\ell = 3$, |m| = 2 harmonics. We sampled the individual masses and spin components using a uniform distribution. The right ascension and declination are sampled uniformly on a solid angle of a sphere. The polar angle, θ , covers the range $\theta \in [-\pi/2, \pi/2]$, while the orbital inclination is sampled using a sin(inclination)-distribution. The coalescence phase and waveform polarization are both uniformly sampled covering the range $[0, 2\pi)$. We created three non-overlapping sets, namely, 2.4M waveforms for training, 300k waveforms for validation, and 300k waveforms for testing.

Sensitivity of detectors. We used the PSD aligo_O4high.txt to model the sensitivity of advanced LIGO detectors, and avirgo_O5low_NEW.txt for advanced Virgo §, 9]. We used this approach to ensure that all detectors in the array have comparable sensitivity for signal detection.

Data curation. We used PyCBC[12] to produce IMRPhenomXPHMIveforms, and to produce Gaussian noise. Both modeled waveforms and Gaussian noise were whitened with the PSDs described above, and then added linearly to simulate events with a broad range of signal-to-noise ratios (SNRs). Given the sparsity of gravitational wave observations, we prepared our training sets so that 70%

of samples contain only pure noise (negative samples), while 30% contain signals contaminated with noise (positive samples). Negative samples consist of 1s-long segments of pure synthetic noise labeled as 0s. To generate positive samples, we truncate a whitened signal and consider only the 0.5s before merger. We set the label for positive samples to be 1 only during the 0.5s before merger, while the rest of the signal will be set to 0. This is done because our AI models respond sharply to the presence of black hole merger signals in the vicinity of the merger event.

AI model architecture. We consider the model architecture introduced in Reference [13], which combines a hybrid dilated convolution network (HDCN) [14] block, and a graph neural network (GNN) [15–19] block. The HDCN block is used to model temporal properties of gravitational wave signals, while the GNN block captures geometrical properties of the three detector network LHV. We illustrate the model structure in Figure 1.

Each of the three distinct HDCN blocks produces processed embeddings for their respective channels. approach This critical as it allows the preservation of each detector's unique information, which is essential for the subsequent GNN block. During this phase, the data traverse through a series of dilated convolution layers, each having varied dilation rates which are used to achieve exponential expansion in the receptive field relative to the number

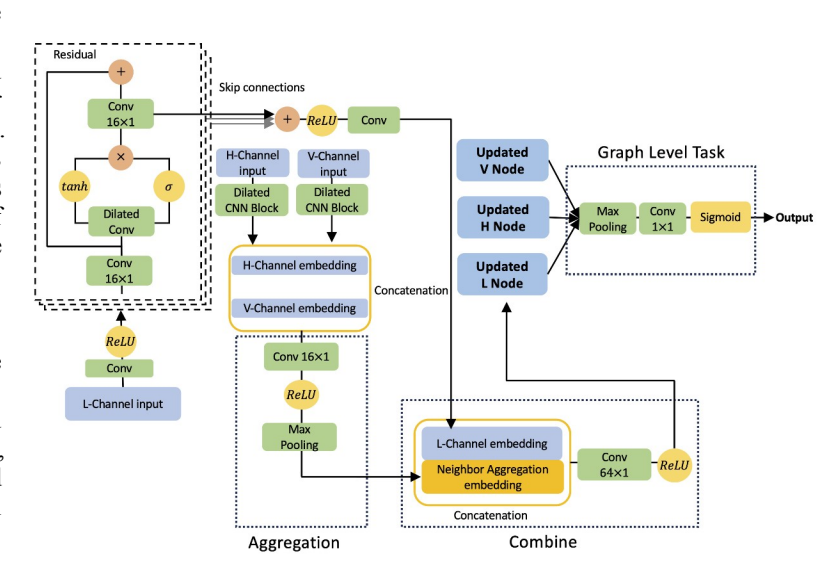


Figure 1: Model structure including the HDCN and GNN blocks.

of layers. The output of 3 blocks will be used as GNN node inputs. For every target node, the GNN block performs both an Aggregate and a Combine operation. The layers used for Aggregate and Combine operations are shared among the three nodes. Subsequently, max pooling is employed to amalgamate the embeddings of the three nodes, producing a singular graph-level embedding. Lastly, a Multi-Layer Perceptron (MLP) with sigmoid activation is applied to the graph-level embedding to formulate element-wise predictions. The architecture of the mass estimation model mirrors that of the detection model. The only difference is in the final layer, since we added an additional convolution layer with activation to yield the total mass estimation.

Training methodology. We trained our AI models within 22 hrs using 96 NVIDIA V100 GPUs at the Summit supercomputer at Oak Ridge National Laboratory. For the purpose of distributed training, we employed Horovod [20]. We used curriculum learning, methodically lowering the SNR to the targeted range. This approach facilitates more efficient and expedited convergence by initially exposing the model to simpler examples. We initiated the learning rate at 1e-3, and halved it if no improvements were observed over three consecutive epochs. To handle our large training sets, we used the LAMB21] optimizer, since it provides adaptivity and efficiency in the training process.

3 Results

AI models raw output. Our AI classifiers produce outputs in the form of element-wise probabilities, indicating the likelihood of each data point being part of a gravitational wave.

Post-processing analysis. AI outputs require further refinement to produce final detection results, since any legitimate signal exist within at least half a second, equivalent to 2048 data points. To

accomplish this, we employ the find_peaks algorithm from SciPy [22]. This algorithm processes the output from our detection models and pinpoints locations that meet the prerequisites of being at least H in height and 2000 in width. Here, H represents a modifiable threshold, pivotal for computing ROC and PR curves. To achieve a minimal False Positive Rate (FPR), we set a high threshold of 0.999999, ensuring that we sustain a substantial True Positive Rate (TPR) simultaneously.

AI performance. To quantify the performance of our AI models, we prepared a year's long test set in which we injected 300,000 IMRPhenomXPkMweforms. We first processed this test using the 3 AI classifiers within 165 seconds using 1024 A100 NVIDIA GPUs in the Polaris supercomputer. The output of these models was then post-processed in 147 seconds using 128 CPU nodes in the ThetaKNL supercomputer.

Figures of merit. We used the post-processed data to compute the ROC AUC and the PR AUC using our ensemble of three AI classifiers with and without total mass predictors. To post-process noise triggers identified by our AI classifiers, we used the total mass predictors. In practice, a filter is applied that considers total masses greater than $5M_{\odot}$ as potential events and disregards those below as noise. This threshold is significantly beneath the range of total masses used during training. The final mass estimation is derived by averaging the outputs of our 2 total mass predictors. To create the ROC curve, we computed the true positive rate against the false positive rate as estimated from the output of our AI ensembles when they process a year-long test set for the HLV network. We injected 300,000 modeled waveforms in this test set, and quantified how accurately our AI ensembles correctly identified injected signals, and discarded other noise anomalies. To produce the PR curve, we consider that PR = TP/ (TP + FP), where TP and FP stand for True Positives and False Positives, respectively. Results for the ROC AUC and the PR AUC are presented in Figure 2. We present the false positive results with different threshold H in Table 1.

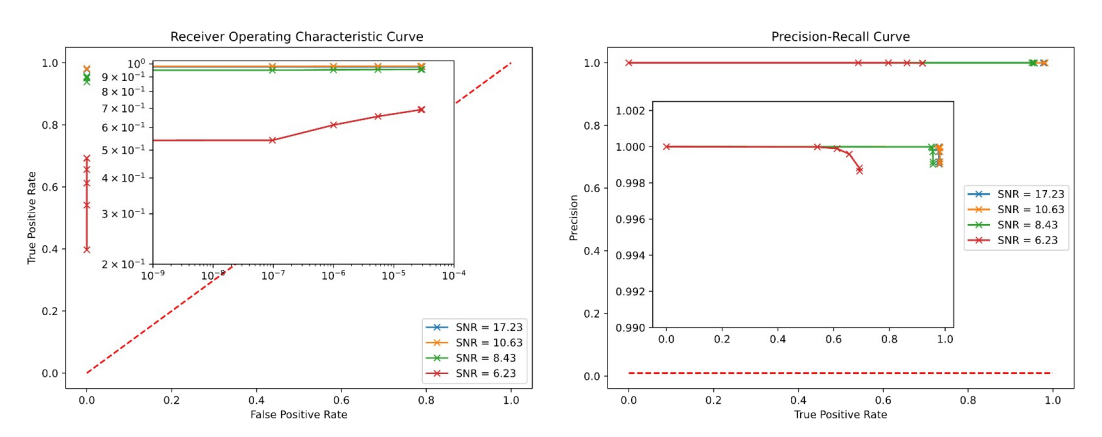


Figure 2: Receiver Operating Characteristic curve (left), and Precision Recall curve (right) for an ensemble of 3 classifiers and 2 mass predictors. Results are shown for a year's long test set in which we injected 300,000 higher order mode waveforms.

A positive signal detection is only declared when there is unanimous agreement among all AI classifiers, else it is classified as a noise anomaly or pure noise. This method of consensus aids in minimizing the FPR, which is crucial for practical applications, ensuring that the detected signals are indeed representative of true events. This approach also provides a rapid estimate of the total mass of potential gravitational wave sources.

Threshold H	Ensemble w/o mass estimation # FP/year FPR		Ensemble w/ mass estimation # FP/year FPR	
0.999999	3	9.65e-8	7	6.43e-8
0.99999	31	9.97e-7	19	6.11e-7
0.9999	170	5.47e-6	80	2.57e-6
0.99	876	2.82e-5	244	7.84e-6
0.9	913	2.94e-5	281	9.03e-6

Table 1: False positive results for different height thresholds, H, and different model ensembles.

A note on AI inference. Though we have developed a framework for hyper efficient, distributed AI inference, our open source AI ensemble may be readily used to process an entire month of data within 1 hour using a single NVIDIA V100 GPU.

4 Conclusions

We introduced a novel AI ensemble of classifiers and predictors that consist of spatiotemporal-graph models that can process gravitational wave data from a three detector network faster than real-time with a single GPU. To the best of our knowledge, these AI models are the first of their kind in the literature that have been trained to search for and find higher order gravitational wave modes that describe quasi-circular, spinning, non-precessing binary black hole mergers.

We quantified the performance of these models by processing a year's long test set within 5 minutes using supercomputers housed at the ALCF, and found that they provide state-of-the-art signal detection accuracy, and only two false positives per year of searched data. The software and computational resources we have developed in this article will be used in future work to train similar AI models using gravitational wave data from the Gravitational Wave Open Science Center [10]. We also plan on improving the scalability of our distributed training methods to further reduce time-to-solution in high performance computing platforms.

Acknowledgments and Disclosure of Funding

This work was supported by Laboratory Directed Research and Development (LDRD) funding from Argonne National Laboratory, provided by the Director, Office of Science, of the U.S. Department of Energy under Contract No. DE-AC02-06CH11357. E.A.H. and M.T. gratefully acknowledge support from National Science Foundation awards OAC-1931561 and OAC-2209892. This work was supported in part by the Diaspora project funded by the U.S. Department of Energy under Contract DE-AC02-06CH11357. This research used resources of the Argonne Leadership Computing Facility, which is a DOE Office of Science User Facility supported under Contract DE-AC02-06CH11357. This research used the Delta advanced computing and data resource which is supported by the National Science Foundation (award OAC 2005572) and the State of Illinois. Delta is a joint effort of the University of Illinois at Urbana-Champaign and its National Center for Supercomputing Applications.

References

- Y. LeCun, Y. Bengio, and G. Hinton, "Deep learning," *Nature*, vol. 521, no. 7553, pp. 436–444, 2015.
- [2] M. Krenn, R. Pollice, S. Y. Guo, M. Aldeghi, A. Cervera-Lierta, P. Friederich, G. dos Passos Gomes, F. Häse, A. Jinich, A. Nigam, Z. Yao, and A. Aspuru-Guzik, "On scientific understanding with artificial intelligence," *Nature Reviews Physics*, vol. 4, pp. 761–769, Dec. 2022.
- [3] A. Davies, P. Veličković, L. Buesing, S. Blackwell, D. Zheng, N. Tomašev, R. Tanburn, P. Battaglia, C. Blundell, A. Juhász, M. Lackenby, G. Williamson, D. Hassabis, and P. Kohli, "Advancing mathematics by guiding human intuition with ai," *Nature*, vol. 600, pp. 70–74, 12 2021.
- [4] E. A. Huerta, G. Allen, I. Andreoni, J. M. Antelis, E. Bachelet, G. B. Berriman, F. B. Bianco, R. Biswas, M. Carrasco Kind, K. Chard, M. Cho, P. S. Cowperthwaite, Z. B. Etienne, M. Fishbach, F. Forster, D. George, T. Gibbs, M. Graham, W. Gropp, R. Gruendl, A. Gupta, R. Haas, S. Habib, E. Jennings, M. W. G. Johnson, E. Katsavounidis, D. S. Katz, A. Khan, V. Kindratenko, W. T. C. Kramer, X. Liu, A. Mahabal, Z. Marka, K. McHenry, J. M. Miller, C. Moreno, M. S. Neubauer, S. Oberlin, A. R. Olivas, D. Petravick, A. Rebei, S. Rosofsky, M. Ruiz, A. Saxton, B. F. Schutz, A. Schwing, E. Seidel, S. L. Shapiro, H. Shen, Y. Shen, L. P. Singer, B. M. Sipocz, L. Sun, J. Towns, A. Tsokaros, W. Wei, J. Wells, T. J. Williams, J. Xiong, and Z. Zhao, "Enabling real-time multi-messenger astrophysics discoveries with deep learning," *Nature Reviews Physics*, vol. 1, pp. 600–608, Oct. 2019.

- [5] E. Cuoco, J. Powell, M. Cavaglià, K. Ackley, M. Bejger, C. Chatterjee, M. Coughlin, S. Coughlin, P. Easter, R. Essick, H. Gabbard, T. Gebhard, S. Ghosh, L. Haegel, A. Iess, D. Keitel, Z. Marka, S. Marka, F. Morawski, T. Nguyen, R. Ormiston, M. Puerrer, M. Razzano, K. Staats, G. Vajente, and D. Williams, "Enhancing Gravitational-Wave Science with Machine Learning," *Mach. Learn. Sci. Tech.*, vol. 2, no. 1, p. 011002, 2021.
- [6] E. A. Huerta and Z. Zhao, "Advances in Machine and Deep Learning for Modeling and Real-Time Detection of Multi-messenger Sources," in *Handbook of Gravitational Wave Astronomy*, p. 47, Springer, Singapore, 2021.
- [7] E. A. Huerta, A. Khan, X. Huang, M. Tian, M. Levental, R. Chard, W. Wei, M. Heflin, D. S. Katz, V. Kindratenko, D. Mu, B. Blaiszik, and I. Foster, "Accelerated, scalable and reproducible AI-driven gravitational wave detection," *Nature Astronomy*, vol. 5, pp. 1062–1068, July 2021.
- [8] B. P. Abbott, R. Abbott, T. D. Abbott, S. Abraham, F. Acernese, K. Ackley, C. Adams, V. B. Adya, C. Affeldt, M. Agathos, K. Agatsuma, N. Aggarwal, O. D. Aguiar, L. Aiello, A. Ain, P. Ajith, T. Akutsu, G. Allen, A. Allocca, M. A. Aloy, P. A. Altin, A. Amato, A. Ananyeva, S. B. Anderson, W. G. Anderson, M. Ando, S. V. Angelova, S. Antier, S. Appert, K. Arai, K. Arai, Y. Arai, S. Araki, A. Araya, M. C. Araya, J. S. Areeda, M. Arène, N. Aritomi, N. Arnaud, K. G. Arun, S. Ascenzi, G. Ashton, Y. Aso, S. M. Aston, P. Astone, F. Aubin, P. Aufmuth, K. AultONeal, C. Austin, V. Avendano, A. Avila-Alvarez, S. Babak, P. Bacon, F. Badaracco, M. K. M. Bader, S. W. Bae, Y. B. Bae, L. Baiotti, R. Bajpai, P. T. Baker, F. Baldaccini, G. Ballardin, S. W. Ballmer, S. Banagiri, J. C. Barayoga, S. E. Barclay, B. C. Barish, D. Barker, K. Barkett, S. Barnum, F. Barone, B. Barr, L. Barsotti, M. Barsuglia, D. Barta, J. Bartlett, M. A. Barton, I. Bartos, R. Bassiri, A. Basti, M. Bawaj, J. C. Bayley, M. Bazzan, B. Bécsy, M. Bejger, I. Belahcene, A. S. Bell, D. Beniwal, B. K. Berger, G. Bergmann, S. Bernuzzi, J. J. Bero, C. P. L. Berry, D. Bersanetti, A. Bertolini, J. Betzwieser, R. Bhandare, J. Bidler, I. A. Bilenko, S. A. Bilgili, G. Billingsley, J. Birch, R. Birney, O. Birnholtz, S. Biscans, S. Biscoveanu, A. Bisht, M. Bitossi, M. A. Bizouard, J. K. Blackburn, C. D. Blair, D. G. Blair, R. M. Blair, S. Bloemen, N. Bode, M. Boer, Y. Boetzel, G. Bogaert, F. Bondu, E. Bonilla, R. Bonnand, P. Booker, B. A. Boom, C. D. Booth, R. Bork, V. Boschi, S. Bose, K. Bossie, V. Bossilkov, J. Bosveld, Y. Bouffanais, A. Bozzi, C. Bradaschia, P. R. Brady, A. Bramley, M. Branchesi, J. E. Brau, T. Briant, J. H. Briggs, F. Brighenti, A. Brillet, M. Brinkmann, V. Brisson, P. Brockill, A. F. Brooks, D. A. Brown, D. D. Brown, S. Brunett, A. Buikema, T. Bulik, H. J. Bulten, A. Buonanno, D. Buskulic, C. Buy, R. L. Byer, M. Cabero, L. Cadonati, G. Cagnoli, C. Cahillane, J. C. Bustillo, T. A. Callister, E. Calloni, J. B. Camp, W. A. Campbell, M. Canepa, K. Cannon, K. C. Cannon, H. Cao, J. Cao, E. Capocasa, F. Carbognani, S. Caride, M. F. Carney, G. Carullo, J. C. Diaz, C. Casentini, S. Caudill, M. Cavaglià, F. Cavalier, R. Cavalieri, G. Cella, P. Cerdá-Durán, G. Cerretani, E. Cesarini, O. Chaibi, K. Chakravarti, S. J. Chamberlin, M. Chan, M. L. Chan, S. Chao, P. Charlton, E. A. Chase, E. Chassande-Mottin, D. Chatterjee, M. Chaturvedi, K. Chatziioannou, B. D. Cheeseboro, C. S. Chen, H. Y. Chen, K. H. Chen, X. Chen, Y. Chen, Y. R. Chen, H. P. Cheng, C. K. Cheong, H. Y. Chia, A. Chincarini, A. Chiummo, G. Cho, H. S. Cho, M. Cho, N. Christensen, H. Y. Chu, Q. Chu, Y. K. Chu, S. Chua, K. W. Chung, S. Chung, G. Ciani, A. A. Ciobanu, R. Ciolfi, F. Cipriano, A. Cirone, F. Clara, J. A. Clark, P. Clearwater, F. Cleva, C. Cocchieri, E. Coccia, P. F. Cohadon, D. Cohen, R. Colgan, M. Colleoni, C. G. Collette, C. Collins, L. R. Cominsky, M. Constancio, L. Conti, S. J. Cooper, P. Corban, T. R. Corbitt, I. Cordero-Carrión, K. R. Corley, N. Cornish, A. Corsi, S. Cortese, C. A. Costa, R. Cotesta, M. W. Coughlin, S. B. Coughlin, J. P. Coulon, S. T. Countryman, P. Couvares, P. B. Covas, E. E. Cowan, D. M. Coward, M. J. Cowart, D. C. Coyne, R. Coyne, J. D. E. Creighton, T. D. Creighton, J. Cripe, M. Croquette, S. G. Crowder, T. J. Cullen, A. Cumming, L. Cunningham, E. Cuoco, T. D. Canton, G. Dálya, S. L. Danilishin, S. D'Antonio, K. Danzmann, A. Dasgupta, C. F. Da Silva Costa, L. E. H. Datrier, V. Dattilo, I. Dave, M. Davier, D. Davis, E. J. Daw, D. DeBra, M. Deenadayalan, J. Degallaix, M. De Laurentis, S. Deléglise, W. D. Pozzo, L. M. DeMarchi, N. Demos, T. Dent, R. De Pietri, J. Derby, R. De Rosa, C. De Rossi, R. DeSalvo, O. de Varona, S. Dhurandhar, M. C. Díaz, T. Dietrich, and L. D. Fiore, "Prospects for observing and localizing gravitational-wave transients with advanced ligo, advanced virgo and kagra," Living Reviews in Relativity, vol. 23, no. 1, p. 3, 2020.
- [9] LIGO Document Control Center Portal, "Noise curves used for Simulations in the update of the Observing Scenarios Paper," 2022. https://dcc.ligo.org/LIGO-T2000012/public .

- [10] R. Abbott *et al.*, "Open Data from the Third Observing Run of LIGO, Virgo, KAGRA, and GEO," *Astrophys. J. Suppl.*, vol. 267, no. 2, p. 29, 2023.
- [11] G. Pratten, C. García-Quirós, M. Colleoni, A. Ramos-Buades, H. Estellés, M. Mateu-Lucena, R. Jaume, M. Haney, D. Keitel, J. E. Thompson, and S. Husa, "Computationally efficient models for the dominant and subdominant harmonic modes of precessing binary black holes," *Phys. Rev. D*, vol. 103, p. 104056, May 2021.
- [12] A. H. Nitz, I. W. Harry, D. A. Brown, C. M. Biwer, J. L. Willis, T. Dal Canton, C. D. Capano, L. P. Pekowsky, T. Dent, A. R. Williamson, G. S. Davies, S. De, M. Cabero, B. Machenschalk, P. Kumar, S. Reyes, D. MacLeod, D. Finstad, F. Pannarale, T. Massinger, S. Kumar, M. Tapai, L. Singer, S. Khan, S. Fairhurst, A. Nielsen, and S. Singh, "PyCBC. Free and open software to study gravitational waves," 2021.
- [13] M. Tian, E. A. Huerta, and H. Zheng, "Physics-inspired spatiotemporal-graph AI ensemble for gravitational wave detection," *arXiv e-prints*, p. arXiv:2306.15728, June 2023.
- [14] A. van den Oord, S. Dieleman, H. Zen, K. Simonyan, O. Vinyals, A. Graves, N. Kalchbrenner, A. Senior, and K. Kavukcuoglu, "WaveNet: A Generative Model for Raw Audio," in *9th ISCA Speech Synthesis Workshop*, pp. 125–125, 2016.
- [15] J. Bruna, W. Zaremba, A. Szlam, and Y. LeCun, "Spectral networks and locally connected networks on graphs," arXiv preprint arXiv:1312.6203, 2013.
- [16] J. Gilmer, S. S. Schoenholz, P. F. Riley, O. Vinyals, and G. E. Dahl, "Neural message passing for quantum chemistry," in *International conference on machine learning*, pp. 1263–1272, PMLR, 2017.
- [17] W. Hamilton, Z. Ying, and J. Leskovec, "Inductive representation learning on large graphs," in *Advances in Neural Information Processing Systems* (I. Guyon, U. V. Luxburg, S. Bengio, H. Wallach, R. Fergus, S. Vishwanathan, and R. Garnett, eds.), vol. 30, Curran Associates, Inc., 2017.
- [18] P. Velickovic, G. Cucurull, A. Casanova, A. Romero, P. Lio, Y. Bengio, et al., "Graph attention networks," stat, vol. 1050, no. 20, pp. 10–48550, 2017.
- [19] K. Xu, W. Hu, J. Leskovec, and S. Jegelka, "How powerful are graph neural networks?," *arXiv* preprint arXiv:1810.00826, 2018.
- [20] A. Sergeev and M. D. Balso, "Horovod: fast and easy distributed deep learning in TensorFlow," arXiv preprint arXiv:1802.05799, 2018.
- [21] Y. You, J. Li, S. Reddi, J. Hseu, S. Kumar, S. Bhojanapalli, X. Song, J. Demmel, K. Keutzer, and C.-J. Hsieh, "Large batch optimization for deep learning: Training bert in 76 minutes," *arXiv preprint arXiv:1904.00962*, 2019.
- [22] P. Virtanen, R. Gommers, T. E. Oliphant, M. Haberland, T. Reddy, D. Cournapeau, E. Burovski, P. Peterson, W. Weckesser, J. Bright, S. J. van der Walt, M. Brett, J. Wilson, K. J. Millman, N. Mayorov, A. R. J. Nelson, E. Jones, R. Kern, E. Larson, C. J. Carey, İ. Polat, Y. Feng, E. W. Moore, J. VanderPlas, D. Laxalde, J. Perktold, R. Cimrman, I. Henriksen, E. A. Quintero, C. R. Harris, A. M. Archibald, A. H. Ribeiro, F. Pedregosa, P. van Mulbregt, and SciPy 1.0 Contributors, "SciPy 1.0: Fundamental Algorithms for Scientific Computing in Python," *Nature Methods*, vol. 17, pp. 261–272, 2020.